Modern Chemistry
2026, Vol. 14, No. 4, pp. 120–140
https://doi.org/10.11648/j.mc.20261404.13

Research Article

Conceptual DFT Study of the Reactivity of Secondary Ketimine Schiff Bases: Influence of Substituents on Electronic Properties and Reactive Sites

Niamké Jean Baptiste Kangah[1], Siriki Doumbia[1], Clémence Ingrid Blénou É[2, 4], Georges Stephane Dembélé[1, 2], Wawohinlin Patrice Ouattara[1], Bibata Konaté[1, 2], Nanou Tieba Tuo[3], Mamadou Guy Richard Koné[1, 2, *], Charles Guillaume Kodjo[1]

[1]Laboratory of Thermodynamics and Physico-Chemistry of the Environment, Nangui Abrogoua University, Abidjan, Ivory Coast

[2]Ivorian Disease Modeling Research Group (GIR2M), Nangui Abrogoua University, Abidjan, Ivory Coast

[3]Department of Training and Research in Chemical and Agro-Food Engineering, Félix Houphouet Boigny National Polytechnic Institute, Yamoussoukro, Ivory Coast

[4]Department of Physics and Chemistry, Alassane Ouattara University, Bouaké, Ivory Coast

Abstract

Secondary ketimine Schiff bases constitute an important class of nitrogen-containing compounds whose electronic properties and reactivity are strongly influenced by their molecular structures and substituents. In this study, we theoretically investigate the effects of hydroxyl, methoxy, and methyl substituents on the electronic properties and reactivity of six secondary ketimines. The calculations were performed within the framework of Density Functional Theory (DFT) using the B3LYP functional and the 6-311G (d, p) basis set, following full geometry optimization. The analysis was based on frontier molecular orbitals, namely the Highest Occupied Molecular Orbital (HOMO) and the Lowest Unoccupied Molecular Orbital (LUMO), global reactivity descriptors, Fukui functions, dual descriptors, Natural Population Analysis (NPA), and Molecular Electrostatic Potential (MEP) surfaces. The results show that the six compounds exhibit relatively similar HOMO–LUMO energy gaps, ranging from 4.112 to 4.201 eV, indicating comparable electronic characteristics. The local reactivity analysis reveals a clear differentiation among the reactive sites within the molecules. The nitrogen atoms of the azomethine group and certain oxygen atoms emerge as preferential sites for interactions with electrophilic species, whereas the carbon atom located between the two nitrogen atoms exhibits a pronounced electrophilic character. These findings highlight the influence of substituents on the electronic distribution and provide useful insights into the understanding and prediction of the reactivity of secondary ketimines.

Keywords

Conceptual DFT, Schiff Bases, Secondary Ketimines, Fukui Functions, Molecular Reactivity, NPA

*Correspondence: Mamadou Guy Richard Koné (guyrichardkone@gmail.com)

Received: 23 September 2026; **Accepted:** 4 October 2026; **Published:** 23 November 2026

Copyright: © The Author(s), 2026. Published by Science Publishing Group. This is an **Open Access** article, distributed under the terms of the Creative Commons Attribution 4.0 License (http://creativecommons.org/licenses/by/4.0/), which permits unrestricted use, distribution and reproduction in any medium, provided the original work is properly cited.

1. Introduction

Schiff bases are an important class of nitrogen-containing organic compounds characterized by the presence of an azomethine group, usually represented by the C=N functionality. Their structural diversity and the possibility of tuning their electronic properties through substituent modification have made them attractive in several areas, including organic chemistry, coordination chemistry, materials science, and medicinal chemistry [1-3]. Recent studies continue to highlight the broad potential of Schiff bases in biological, pharmaceutical, analytical, and coordination applications [2-5].

Among this family of compounds, secondary ketimines are of particular interest because of the electronic environment around their azomethine group. The nature, number, and position of substituents on the aromatic rings can modify the electron-density distribution, frontier molecular orbital energies, and, consequently, the reactivity of specific molecular sites [5]. Recent DFT studies have shown that structural modifications of Schiff bases can significantly affect HOMO and LUMO energies, energy gaps, and other electronic properties [3-5]. However, a substantial part of the available literature focuses either on individual molecules or on specific applications, such as metal-ion complexation, sensing, biological activity, or corrosion inhibition [3-5].

Density Functional Theory (DFT) has become a widely used tool for investigating the electronic structure and molecular properties of Schiff bases. Within the framework of frontier molecular orbital theory, the Highest Occupied Molecular Orbital (HOMO) and the Lowest Unoccupied Molecular Orbital (LUMO) provide useful information about the relative electron-donating and electron-accepting abilities of a molecule [6, 7]. Conceptual Density Functional Theory (CDFT) provides a broader framework by connecting electronic structure with chemical reactivity through global descriptors such as chemical potential, electronegativity, hardness, softness, and electrophilicity [7, 8].

Global descriptors, however, provide an overall picture of molecular reactivity and cannot, by themselves, identify the specific sites that are most likely to participate in chemical interactions. Fukui functions, introduced within the framework of CDFT, provide information on the local response of electron density to changes in the number of electrons [8]. The electrophilicity index proposed by Parr et al. is a global descriptor of the ability of a chemical species to accept electron density [10]. In addition, the dual descriptor, derived from the difference between the Fukui functions, provides a useful way to distinguish regions with predominantly nucleophilic or electrophilic character and to investigate local selectivity [11, 12].

Recent studies on Schiff bases have demonstrated the usefulness of combining these approaches. For example, studies integrating experimental characterization with DFT calculations have used frontier molecular orbitals, atomic charges, molecular electrostatic potential surfaces, and reactivity descriptors to interpret the electronic properties of Schiff bases and their metal complexes [4, 14]. These investigations show that structural modifications can influence electron-density distribution, electron-donating and electron-accepting properties, and the location of potentially reactive sites. However, most of these studies have focused on a limited number of molecular structures and have addressed specific applications, such as metal-ion sensing or biological activity [4, 14].

Despite these advances, the systematic effect of hydroxyl (–OH), methoxy (–OCH_3), and methyl (–CH_3) substituents on the global electronic properties and local reactivity of a structurally related series of secondary ketimines remains insufficiently explored. Most published studies have focused on individual structures, compounds designed for a particular application, or systems in which several structural modifications are introduced simultaneously [3, 4, 14].

In particular, previous studies have not clearly established, within a common molecular framework, to what extent the progressive introduction of –OH, –OCH_3, and –CH_3 groups affects not only the magnitude of the electronic descriptors but also the identity and location of the main reactive sites. It also remains unclear whether the trends observed from global descriptors, such as the HOMO–LUMO gap, hardness, softness, and electrophilicity, are consistently reflected in local descriptors such as Fukui functions and the dual descriptor, as well as in NPA charges and molecular electrostatic potential distributions.

This issue is particularly relevant for secondary ketimines because the effect of a substituent depends not only on its intrinsic electronic properties but also on its position within the molecular framework and its interaction with the azomethine group. A direct comparison of closely related molecular structures is therefore needed to distinguish substituent-specific effects from changes associated with broader structural differences.

A systematic comparison of molecules belonging to the same structural family can provide a clearer understanding of the structure–property–reactivity relationships governing secondary ketimines. Combining frontier molecular orbitals, global descriptors, and local reactivity descriptors provides complementary information on their electronic behavior. Natural Population Analysis (NPA) offers additional insight into atomic charge distribution, while molecular electrostatic potential (MEP) surfaces provide a visual representation of electron-rich and electron-deficient regions [4, 5, 12].

Within this framework, an integrated CDFT-based approach is particularly useful for examining substituent effects under consistent computational conditions and for identifying reactivity trends shared across a molecular series rather than focusing only on isolated compounds [6, 7].

The main objective of this study is therefore to systemati-

cally investigate the influence of hydroxyl, methoxy, and methyl substituents on the electronic properties and reactivity of six secondary ketimine Schiff bases. More specifically, the study aims to:

1) compare the HOMO and LUMO energies and HOMO–LUMO gaps of the six compounds;
2) evaluate the effect of the substituents on the main global reactivity descriptors;
3) identify the principal nucleophilic and electrophilic sites using Fukui functions and the dual descriptor;
4) determine whether the structural modifications mainly affect the magnitude of reactivity or also change the location of the main reactive sites; and
5) assess the consistency between the predictions obtained from local reactivity descriptors, NPA charges, and MEP surfaces.

The originality of this work lies in the systematic comparison of six closely related secondary ketimines within a single computational framework, allowing the individual and combined effects of –OH, $–OCH_3$, and $–CH_3$ substituents to be examined under comparable conditions. Whereas previous studies have mainly focused on individual Schiff bases or specific applications [3, 4, 13], the present work seeks to establish general trends linking substitution, electronic structure, and local reactivity across a structurally related series.

This approach is expected to provide a deeper understanding of the relationship between molecular structure, electron-density distribution, and local chemical reactivity in secondary ketimine Schiff bases and to provide a useful theoretical basis for future experimental and application-oriented studies.

2. Computational Details

2.1. Molecular Systems

Six secondary ketimine Schiff bases bearing different substituents on their aromatic rings were selected for this study. The molecular structures of the investigated compounds are presented in Figure 1 and Figure 1.

The series includes hydroxyl (–OH), methoxy ($–OCH_3$), and methyl ($–CH_3$) substituents, introduced onto the phenyl and pyridyl rings to assess their effects on the electronic distribution and molecular reactivity. The six investigated compounds are listed below:

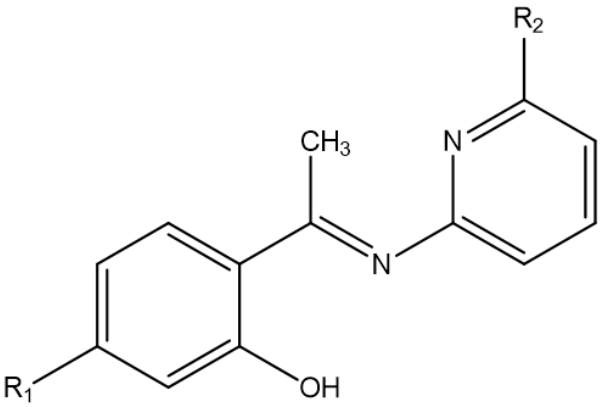

Figure 1. *General structure of the molecular skeleton of secondary cetimine-type Schiff bases.*

Table 1. *Various substituents associated with the molecular skeleton of secondary cetimine-type Schiff bases.*

Molecule 1:	R1=H R2=H: (E)-2-(1-(pyridin-2-ylimino)ethyl)phenol
Molecule 2:	R1=OH R2=H: (E)-4-(1-(pyridin-2-ylimino)ethyl)benzene-1,3-diol
Molecule 3:	R1=O-CH3 R2=H: (E)-5-methoxy-2-(1-(pyridin-2-ylimino)ethyl)phenol
Molecule 4:	R1=H R2=CH3: (E)-2-(1-((6-methylpyridin-2-yl)imino)ethyl)phenol
Molecule 5:	R1=OH R2=CH3: (E)-4-(1-((6-methylpyridin-2-yl)imino)ethyl)benzene-1,3-diol
Molecule 6:	R1=O-CH3 R2=CH3: (E)-5-methoxy-2-(1-((6-methylpyridin-2-yl)imino)ethyl)phenol

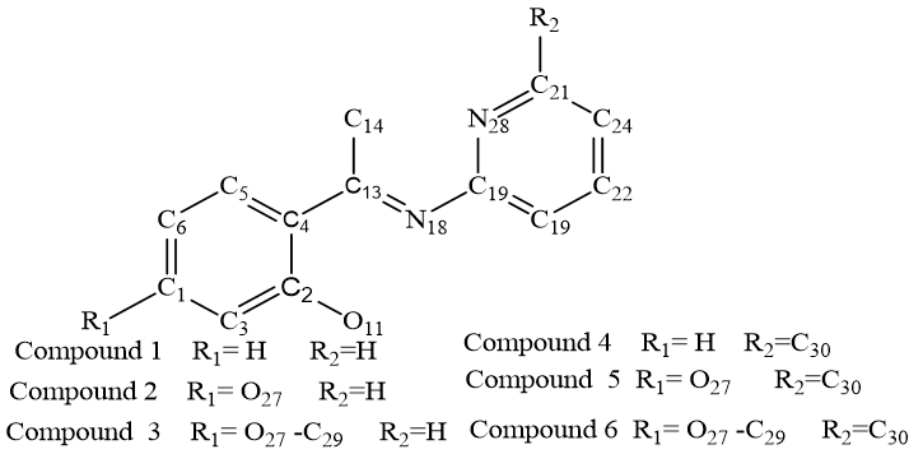

Figure 2. *Molecular structures of the six secondary ketimine Schiff base compounds.*

The initial structures were constructed from the corresponding chemical formulas and subsequently subjected to full geometry optimization. Particular attention was paid to the azomethine C=N group, which represents a key structural feature in the analysis of the electronic properties and reactivity of these molecules [1, 4].

2.2. Computational Methodology

The calculations were performed within the framework of density functional theory (DFT), using the hybrid B3LYP functional in combination with the 6-311G (d, p) basis set. All calculations were carried out using the Gaussian 09 software package, Revision D.01 [15].

For each compound, a full molecular geometry optimization was performed without imposing any geometrical constraints. The optimized neutral structures were then used for the frontier-orbital analysis. Condensed Fukui functions were obtained from the natural atomic populations of the neutral, anionic, and cationic electronic states, as defined in Section 2.4. Natural population analysis (NPA) was used to provide the atomic populations required for the condensed local descriptors and to analyse the resulting charge distribution. The manuscript should retain the convergence criteria, charge and multiplicity, and the precise treatment of the charged states used in the original Gaussian input/output files when preparing the final submission, since these parameters are not specified in the present text.

The analysis of these orbitals provides valuable information about the relative electron-donating and electron-accepting abilities of the molecules [5]. Previous computational studies have also demonstrated the usefulness of DFT calculations for characterizing the structural, electronic, vibrational, and optical properties of various molecular systems [6, 7].

The energy difference between the frontier molecular orbitals was calculated using the following expression:

$$\Delta_{E_{gap}} = E_{LUMO} - E_{HOMO} \quad (1)$$

This energy gap was used as a comparative indicator of the electronic structures of the six compounds. Within the framework of conceptual DFT, the frontier orbital energies were also used to estimate the global reactivity descriptors according to the Koopmans approximation [5-7].

In the present study, the electronic properties were further analyzed using Conceptual Density Functional Theory (CDFT). This approach makes it possible to relate the electronic properties of molecular systems to their chemical behavior through various global reactivity descriptors [6, 7].

2.3. Global Reactivity Descriptors

The global reactivity of the molecules was evaluated using several descriptors derived from conceptual DFT (CDFT), including the electronic chemical potential μ, electronegativity χ, chemical hardness η, chemical softness S, and electrophilicity index ω [6-8].

The global reactivity descriptors were calculated from the frontier orbital energies using the Koopmans approximation. The ionization energy *I* and electron affinity *A* were estimated from the HOMO and LUMO energies, respectively, according to the following expressions:

$$I \approx -E_{HOMO} \ \ and \ \ A \approx -E_{LUMO} \quad (2)$$

The use of orbital energies to interpret molecular reactivity is consistent with the frontier molecular orbital approach, which relates electronic structure to chemical reactivity [2, 3]. The electronic chemical potential μ and electronegativity χ were determined using:

$$\mu = -\frac{I+A}{2} \ \ and \ \ \chi = -\mu = \frac{I+A}{2} \quad (3)$$

The chemical hardness η, which characterizes the resistance of a system to changes in its electronic distribution, was calculated as follows:

$$\eta = \frac{I-A}{2} = \frac{E_{LUMO}-E_{HOMO}}{2} \quad (4)$$

The relationship between chemical hardness and softness is one of the fundamental concepts of Pearson's HSAB theory (Hard and Soft Acids and Bases) [16]. These concepts are particularly useful for discussing the relative tendency of chemical species to participate in different interactions according to their hard or soft character.

The global chemical softness, *S*, was obtained from

$$S = \frac{1}{2\eta} \quad (5)$$

Finally, the global electrophilicity index, ω\omegaω, introduced by *Parr et al*., was calculated according to the following expression [9]:

$$\omega = \frac{\mu^2}{2\eta} \quad (6)$$

Electrophilicity is an important descriptor of global molecular reactivity and provides an estimate of the tendency of a molecule to accept electron density [9].

All these descriptors were used to compare the global electronic properties of the six ketimines and to evaluate the influence of the substituent nature on their electronic behavior.

2.4. Local Reactivity Descriptors

To identify the molecular sites that may preferentially participate in chemical interactions, the condensed Fukui functions were calculated from the natural atomic populations [9, 10].

For an atomic site k, the Fukui functions associated with nucleophilic and electrophilic attacks are defined as follows:

$$f_k^+ = q_k(N+1) - q_k(N) \quad and \quad f_k^- = q_k(N) - q_k(N-1) \quad (7)$$

where $q_k(N), q_k(N+1)$ and $q_k(N-1)$ represent the electron populations of site k in the neutral molecule, anionic species, and cationic species, respectively [9].

The f^+ function is used to identify sites that are more susceptible to nucleophilic attack, whereas f^-identifies sites that are more susceptible to electrophilic attack. The condensed functions were obtained from the natural atomic populations of the neutral, anionic, and cationic species according to the definitions given above [7, 9, 10].

The corresponding local softness values were determined from the global softness:

$$S_k^+ = S\ f_k^+ \quad and \quad S_k^- = S\ f_k^- \quad (8)$$

The local electrophilicity indices were also calculated according to:

$$\omega_k^+ = \omega\ f_k^+ \quad and \quad \omega_k^- = \omega\ f_k^- \quad (9)$$

To distinguish the electrophilic and nucleophilic character of the different sites, the dual descriptor was calculated as follows:

$$\Delta f_k = f_k^+ - f_k^- \quad (10)$$

A positive value of Δf_k indicates a relatively electrophilic character at the site under consideration, corresponding to a greater susceptibility to nucleophilic attack. Conversely, a negative value indicates a relatively nucleophilic character, associated with a greater susceptibility to electrophilic attack [10].

The combined use of Fukui functions, local softness, and the dual descriptor provides a more detailed description of the local reactivity of the different atoms in the six molecules [8-10].

2.5. Natural Population Analysis and Molecular Electrostatic Potential

Natural population analysis (NPA) was performed to examine the distribution of electron density within the six molecules. The natural atomic charges obtained from this analysis complement the Fukui functions and dual descriptors by providing information on variations in electron density associated with the different atoms [17].

NPA is particularly useful for the Schiff bases investigated in this study because it makes it possible to examine the influence of substituents on the electronic distribution around the azomethine group, as well as around oxygen and carbon atoms that may participate in chemical interactions.

The Molecular Electrostatic Potential (MEP) surface was also calculated to visualize the spatial distribution of the electrostatic potential around the molecules. Regions of negative electrostatic potential are generally associated with electron-rich areas, whereas regions of positive electrostatic potential correspond to areas that are relatively electron-deficient.

The MEP maps were compared with the results obtained from the local reactivity descriptors in order to assess the consistency of the reactivity predictions [4, 11]. Negative electrostatic potential regions are generally associated with electron-rich areas and may be considered preferentially nucleophilic regions. In contrast, positive potential regions correspond to areas that are relatively electron-deficient and may exhibit electrophilic character.

The MEP maps were therefore compared with the results obtained from the Fukui functions and the dual descriptor to evaluate the consistency among the different approaches used to analyze molecular reactivity [7, 9, 10].

3. Results and Discussion

3.1. Analysis of Frontier Molecular Orbitals

The energies of the frontier molecular orbitals, namely the highest occupied molecular orbital (HOMO) and the lowest unoccupied molecular orbital (LUMO), together with the HOMO–LUMO energy gap ΔE_{gap} (HOMO–LUMO), ionization energy (*I*), and electron affinity (*A*), are presented in Table 2. These parameters make it possible to evaluate certain electronic properties and the potential reactivity of the investigated compounds based on frontier molecular orbital theory and conceptual density functional theory.

Table 2. *Energy descriptors of the investigated compounds in eV.*

Molecules	E_{HOMO}(eV)	E_{LUMO}(eV)	ΔEgap(eV)	I(eV)	A(eV)
1	-6.017	-1.905	4.112	6.017	1.905
2	-5.949	-1.762	4.187	5.949	1.762
3	-5.908	-1.735	4.173	5.908	1.735
4	-5.982	-1.853	4.129	5.982	1.853
5	-5.910	-1.709	4.201	5.910	1.709
6	-5.869	-1.687	4.182	5.869	1.687

The frontier molecular orbitals, HOMO and LUMO, play a central role in interpreting the chemical reactivity of molecules. The HOMO is generally associated with the electron-donating ability of a molecule, whereas the LUMO is related to its electron-accepting capacity. These orbitals can also contribute to the interpretation of Intramolecular Charge Transfer (ICT), as well as to the analysis of certain electronic and optical properties of the investigated systems [17].

A high HOMO energy, that is, a less negative numerical value, generally indicates a greater ability of a molecule to donate electrons. Conversely, a low LUMO energy, corresponding to a more negative value, indicates a greater ability to accept electrons. These trends should nevertheless be interpreted with caution, because actual reactivity also depends on the nature of the reactive sites, the distribution of electron density, the chemical environment, and steric effects.

According to the results presented in Table 2, compound 6 has the highest HOMO energy, with EHOMO = −5.869 eV, whereas compound 1 has the lowest HOMO energy, with EHOMO = −6.017 eV. The increasing order of HOMO energies is therefore:

Compound 6 > Compound 5 > Compound 3 > Compound 2 > Compound 4 > Compound 1

Thus, compound 6 appears to have the greatest relative ability to donate electron density, whereas compound 1 is the least likely to donate an electron within this series.

Regarding the LUMO energies, compound 1 has the lowest value, ELUMO = −1.905 eV, whereas compound 6 has the highest value, ELUMO = −1.687 eV. The increasing order of LUMO energies is as follows:

Compound 1 < Compound 4 < Compound 2 < Compound 3 < Compound 5 < Compound 6

On this basis, compound 1 appears to be the most favorable potential electron acceptor in the series, whereas compound 6 exhibits the lowest relative electron-accepting ability. This trend may be related to the electronic effects of the substituents introduced into the molecular framework of the reference compound. Indeed, substitution can modify the distribution of electron density and consequently influence the energy levels of the frontier orbitals [18].

The six investigated compounds share the same secondary ketimine framework but differ in the nature and position of hydroxyl, methoxy, and methyl substituents. The series should therefore be interpreted as a set of related substitution patterns rather than as a strictly progressive substitution sequence.

The HOMO–LUMO energy gap, defined by the relationship: $\Delta_{E_{gap}} = E_{LUMO} - E_{HOMO}$

is an important indicator of the energy separation between the frontier orbitals. The values calculated for the six compounds are relatively close and are all greater than 4.1 eV. Compound 5 exhibits the largest energy gap, with ΔEgap = 4,201 eV, followed by compound 2 with 4.187 eV and compound 6 with 4.182 eV. Compound 1 has the smallest energy gap, with a value of 4.112 eV, followed by compound 4 with 4.129 eV and compound 3 with 4.173 eV.

The decreasing order of the HOMO–LUMO energy gaps is therefore:

Compound′ 5> Compound′ 2> Compound′ 6> Compound′ 3> Compound′ 4> Compound′ 1

Within the framework of conceptual density functional theory, a relatively large HOMO–LUMO gap is generally associated with greater chemical hardness, lower polarizability, and a reduced ability to undergo electronic reorganization.

Conversely, a smaller gap may be associated with greater electronic flexibility and potentially higher reactivity [19]. In the present series, compound 1, which has the smallest energy gap, may therefore exhibit a greater ability to redistribute its electron density than the other compounds. However, the differences between the calculated values remain relatively small; therefore, it would be excessive to conclude that the compounds exhibit markedly different reactivities based solely on this descriptor.

Furthermore, the HOMO–LUMO gap cannot, by itself, directly predict the biological activity of a molecule. It may provide information about electronic stability, polarizability, and potential reactivity, but biological activity depends on many other factors, including solubility, lipophilicity, metabolic stability, the ability to interact with a biological target, and pharmacokinetic properties. Therefore, the ΔEgap values obtained in this study should be regarded as electronic indicators rather than direct evidence of high biological activity.

The ionization energy (I) represents the energy required to remove an electron from a neutral molecule. Within the approximation used, it is generally estimated as the negative of the HOMO energy:

$$I \approx -E_{HOMO}$$

A high ionization energy indicates that electron removal is more difficult and may be associated with greater resistance to oxidation. Conversely, a low ionization energy indicates a greater tendency toward electron loss and may be related to a greater ability to participate in certain oxidation processes.

According to the values reported in Table 2, compound 1 has the highest ionization energy, with I = 6.017 eV, whereas compound 6 has the lowest value, with I = 5.869 eV. This trend is consistent with the HOMO energies: compound 1, whose HOMO is the lowest, is the least likely to donate an electron, whereas compound 6, whose HOMO is the highest, exhibits a relatively greater tendency toward electron loss.

The electron affinity (A) is associated with the energy variation resulting from the addition of an electron to a neutral molecule. Within the frontier molecular orbital approximation, it is estimated using the relationship: $A \approx -E_{LUMO}$

A high electron affinity generally indicates a greater ability of a molecule to accept an electron. Compound 1 has the highest electron affinity, with A=1.905 eV, whereas compound 6 has the lowest value, with A=1.687 eV. This trend confirms that compound 1 is the most favorable potential electron acceptor among the investigated molecules, whereas compound 6 is the least favored for this type of process.

Overall, the substituted compounds show generally higher HOMO and LUMO energies than the reference structure, accompanied by lower ionization energies and electron affinities. These trends indicate a relative increase in electron-donating character and a decrease in electron-accepting tendency, while the detailed magnitude depends on the specific substitution pattern.

3.2. Global Reactivity Descriptors of the Compounds

Global chemical reactivity descriptors, including the chemical potential μ, electronegativity χ, global chemical hardness η, global softness S, and global electrophilicity index ω, provide further insight into the frontier molecular orbital analysis. These parameters offer information about the general tendency of molecules to donate or accept electrons, as well as their resistance to perturbations in their electronic distribution. The calculated values for the six compounds investigated are summarised in Table 3.

Table 3. *Global chemical reactivity descriptors of the six compounds investigated.*

Compound	μ(eV)	η(eV)	ω(eV)	s(eV^{-1})
1	-3.961	2.056	3.816	0.243
2	-3.856	2.094	3.550	0.239
3	-3.822	2.087	3.500	0.240
4	-3.918	2.065	3.717	0.242
5	-3.810	2.101	3.454	0.238
6	-3.778	2.091	3.413	0.239

Electronic Chemical Potential

The electronic chemical potential, μ, is related to the global electronegativity, χ, through the relationship:

$$\mu = -\chi.$$

This molecular descriptor provides an indication of a molecule's tendency to release electrons. In general, a higher chemical potential is associated with a greater tendency to donate electron density.

A less negative chemical potential generally indicates a relatively greater ability to donate electron density, whereas a more negative value is generally associated with a stronger tendency to retain electrons.

The results presented in Table 3 show that compound 1 has the most negative chemical potential, with a value of μ=−3.961 eV. It is followed by compounds 4, 2, 3, 5, and 6, according to the following order:

Compound 1 < Compound 4 < Compound 2 < Compound 3 < Compound 5 < Compound 6

This order is based on increasing chemical potential values, from the most negative to the least negative.

Compound 6 exhibits the least negative chemical potential, with μ=−3.778 eV. Relative to the other compounds, it may therefore have a slightly greater tendency to donate electron density. However, the chemical potential should not be regarded as an absolute measure of reactivity when considered in isolation. Its interpretation should be complemented by the analysis of chemical hardness, softness, electrophilicity, and local reactivity descriptors.

Global Chemical Hardness

Global chemical hardness, η, measures a molecule's resistance to changes in its electronic distribution.

A high value of η is generally associated with greater resistance to deformation of the electron cloud and a lower tendency for electron-density redistribution. Conversely, a lower value of η may indicate greater electronic flexibility and potentially enhanced reactivity.

According to Table 3, compound 5 has the highest chemical hardness, with η=2.101 eV, whereas compound 1 exhibits the lowest value, with η=2.056 eV.

The decreasing order of chemical hardness is as follows:

Compound 5> Compound 2> Compound 6> Compound 3> Compound 4> Compound 1

Compound 5 can therefore be described as the hardest system in the series, while compound 1 exhibits the lowest hardness. This trend suggests that compound 1 may be slightly more polarizable or more capable of undergoing electron-density redistribution than the other compounds.

Nevertheless, the differences in chemical hardness are relatively small, as the values range from 2.056 to 2.101 eV. These results should therefore be interpreted as relative trends rather than as evidence of major differences in chemical behaviour.

Global Chemical Softness

Global softness, S, is the inverse of chemical hardness and describes the ease with which a molecule's electronic distribution can be perturbed. A higher value of S is generally associated with greater electronic flexibility and a greater tendency to participate in interactions involving charge transfer. The calculated softness values range from 0.238 to 0.243 eV^{-1}. Compound 1 exhibits the highest softness, with S=0.243 eV^{-1}, whereas compound 5 has the lowest value, with S=0.238 eV^{-1}.

The decreasing order of softness is therefore:

Compound 1>Compound 4>Compound 3>Compound 2=Compound 6 > Compound 5

The softness values generally follow the opposite trend to the hardness values, which is consistent with the mathematical relationship between these two descriptors. Thus, compound 1, which exhibits the lowest hardness, also shows the highest softness in the series.

According to the Hard and Soft Acids and Bases (HSAB) theory proposed by Pearson, hard species generally tend to interact preferentially with hard species, whereas soft species tend to interact more favourably with soft species [16]. In the context of the present study, the η and S values can therefore be used to qualitatively discuss the electronic flexibility and potential interactions of the compounds investigated.

Global Electrophilicity Index

The global electrophilicity index, ω, characterises a molecule's ability to accept electron density. A high value of ω generally indicates a strong electron-accepting capability. Accordingly, a molecule with a high electrophilicity index may be considered a more favourable potential electron acceptor than one with a lower value, all other factors being equal.

The values reported in Table 3 show that compound 1 has the highest global electrophilicity index, with ω=3.816 eV. It is followed by compounds 4, 2, 3, 5, and 6. The decreasing order of global electrophilicity is therefore:

Compound 1> Compound 4 > Compound 2 > Compound 3 > Compound 5 > Compound 6

Compound 6 exhibits the lowest electrophilicity index, with ω=3.413 eV. It therefore shows the lowest relative global electron-accepting tendency in the series, whereas compound 1 exhibits the highest relative electrophilic character.

This trend is consistent with the frontier orbital results. Compound 1 has the lowest LUMO energy and the highest electron affinity, which is compatible with its relatively high electrophilicity index. Conversely, compound 6 exhibits the highest LUMO energy and the lowest electron affinity, corresponding to its lower ω value.

Influence of Substituents on the Global Reactivity Descriptors

Variations in the global reactivity descriptors can be related to the electronic effects of the substituents present on the aromatic rings. Hydroxyl (−OH), methoxy ($-OCH_3$), and methyl ($-CH_3$) groups can modify the electron-density distribution through their inductive and resonance effects. In particular, hydroxyl and methoxy groups can exert a resonance-donating effect within the aromatic system, whereas the methyl group primarily exhibits an inductive electron-donating effect. The successive introduction of these substituents may therefore influence the energy levels of the HOMO and LUMO, the ionisation energy, the electron affinity, and, consequently, the global reactivity descriptors.

The results show that, from compound 1 to compound 6, the chemical potential becomes progressively less negative,

increasing from −3.961 to −3.778 eV. This evolution suggests a relative increase in the tendency of the substituted compounds to donate electron density.

At the same time, the electrophilicity index decreases from 3.816 eV for compound 1 to 3.413 eV for compound 6. This decrease indicates a progressive reduction in the overall electron-accepting tendency of the compounds. It is consistent with the increase in LUMO energy and the decrease in electron affinity observed in the preceding analysis.

The chemical hardness and softness descriptors, in contrast, show relatively small variations. Compound 5 is the hardest and least soft compound, whereas compound 1 exhibits the lowest hardness and the highest softness. These results suggest that the substitutions modify the overall electronic reactivity of the molecules without producing substantial changes in their resistance to electronic perturbation.

Overall, the results indicate that compound 1 exhibits the most pronounced global electrophilic character and the highest softness, whereas compound 6 has the least negative chemical potential, the lowest electrophilicity index, and a relatively high chemical hardness. These trends suggest that the introduced substituents progressively enhance the electron-donating character of the compounds while reducing their overall electron-accepting tendency. However, the local reactivity analysis will focus on compounds 1 and 6, which exhibit the most pronounced differences in the global reactivity descriptors.

3.3. Local Reactivity Descriptors of the Compounds

The local reactivity of a chemical species can be investigated using several descriptors, including the Fukui functions f^+ and f^-as well as the dual descriptor Δf. These parameters help identify molecular sites that are more likely to participate in electrophilic or nucleophilic reactions and can also provide valuable insight into regioselectivity.

The Fukui function f^+ is generally associated with changes in the electron density upon the addition of an electron to the system. It therefore provides information about sites that are more likely to accept electron density and, consequently, may be more susceptible to nucleophilic attack. Conversely, the Fukui function f^-, which is derived from changes in electron density upon electron removal, helps identify sites that are more likely to donate electron density and may therefore be preferentially involved in electrophilic attack.

The condensed Fukui functions, denoted as Δf_k, allow the reactivity of different atoms within a molecule to be compared. In general, the site with the highest f_k^+ value is considered the most favourable site for nucleophilic attack, whereas the site with the highest f_k^-value is generally regarded as the most favourable site for electrophilic attack.

A positive value of the dual descriptor Δf_k generally indicates local electrophilic character, associated with a tendency to accept electron density. Conversely, a negative value of Δf_k generally indicates local nucleophilic character, associated with a tendency to donate electron density. This descriptor is particularly useful for investigating the regioselectivity of chemical reactions.

Other local descriptors can also be derived from the Fukui functions, including the local softness indices s_k^+ and s_k^-, as well as the local electrophilicity indices ω_k^+ and ω_k^-. These quantities provide a way to weight the Fukui functions using the global reactivity descriptors.

The molecular electrostatic potential (MEP) is another important tool for investigating local reactivity. It enables the spatial distribution of the electrostatic potential around a molecule to be visualised and helps identify regions that may interact with charged or polarised species. Regions of negative electrostatic potential, commonly represented by warm colours such as red, are generally associated with electron-rich areas and may correspond to nucleophilic sites. Conversely, regions of positive electrostatic potential, commonly represented by cool colours such as blue, correspond to electron-deficient areas and may be associated with electrophilic sites.

3.3.1. Dual Descriptor and Molecular Electrostatic Potential of Compound 1

The local and dual reactivity descriptors of the optimised compound 1 were calculated from the electron populations obtained through Natural Population Analysis (NPA) at the B3LYP/6-311G (d, p) level of theory. The results are summarised in Table 4. The profile of the dual descriptor, Δf, is presented in Figure 3, while the molecular electrostatic potential surface of compound 1 is shown in Figure 4. Nucleophilic sites are represented in red, whereas electrophilic sites are shown in blue.

Moreover, the molecular electrostatic potential (MEP) surface provides a visual representation of the electrostatic potential distribution around the molecule. Red regions correspond to areas of negative electrostatic potential and are therefore electron-rich, making them preferential sites for interactions with electrophilic species. In contrast, blue regions represent areas of positive electrostatic potential and relative electron deficiency, which may favor interactions with nucleophilic species. Intermediate colors, such as yellow and green, indicate regions with intermediate electrostatic potential. The exact color scale depends on the potential range and visualization settings used in the calculations.

Table 4. *Local and dual reactivity descriptors of compound 1 calculated from NPA at the B3LYP/6-311G (d, p) level of theory.*

Atoms	Local descriptors						Dual descriptors		
	f+	f-	S+	S-	ω+	ω-	Δf(r)	ΔS(r)	ΔW(r)
C1	0.159	-0.149	0.076	-0.071	0.566	-0.528	0.308	0.147	1.094
C2	-0.136	0.161	-0.065	0.077	-0.484	0.57	-0.297	-0.142	-1.054
C3	0.192	-0.167	0.091	-0.08	0.68	-0.593	0.358	0.171	1.273
C4	-0.101	0.3	-0.048	0.143	-0.358	1.066	-0.401	-0.192	-1.424
C5	-0.109	0.014	-0.052	0.007	-0.388	0.049	-0.123	-0.059	-0.437
C6	-0.128	0.345	-0.061	0.165	-0.456	1.227	-0.474	-0.226	-1.682
O11	-0.325	0.427	-0.155	0.204	-1.154	1.515	-0.752	-0.359	-2.669
C13	0.107	-0.237	0.051	-0.113	0.381	-0.842	0.344	0.164	1.222
C14	-0.316	0.319	-0.151	0.152	-1.123	1.132	-0.635	-0.303	-2.255
N18	-0.306	0.453	-0.146	0.216	-1.087	1.607	-0.759	-0.362	-2.694
C19	0.166	-0.199	0.079	-0.095	0.589	-0.707	0.365	0.174	1.296
C20	-0.117	0.207	-0.056	0.099	-0.416	0.735	-0.324	-0.155	-1.15
C21	0.056	-0.019	0.027	-0.009	0.199	-0.067	0.075	0.036	0.267
C22	-0.069	0.057	-0.033	0.027	-0.246	0.203	-0.126	-0.06	-0.448
C24	-0.143	0.239	-0.068	0.114	-0.507	0.85	-0.382	-0.183	-1.357
N28	-0.263	0 271	-0.128	-0.132	-1.006	1.036	-0.535	-0.260	-2.042

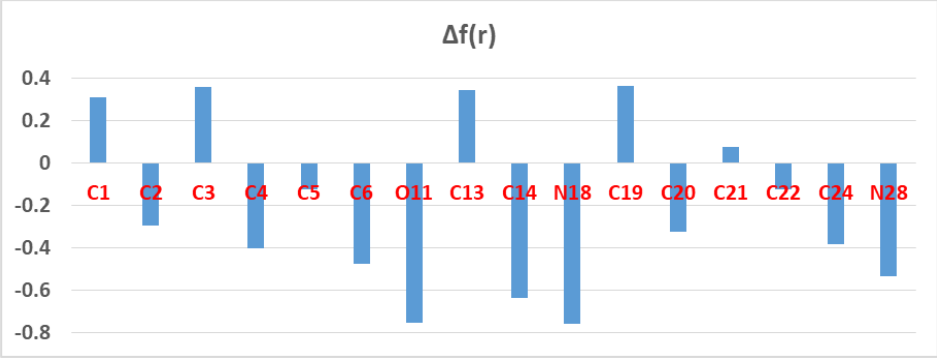

Figure 3. *Dual descriptor (Δf) profile of compound 1.*

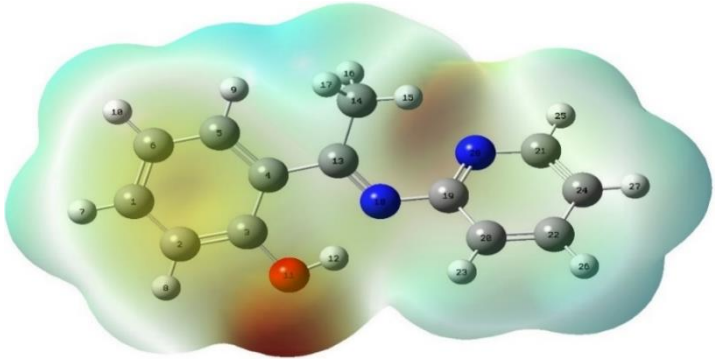

Figure 4. *Molecular electrostatic potential surface of compound 1.*

The most negative Δf values in compound 1 occur at N18 (−0.759), O11 (−0.752), and N28 (−0.535), identifying these atoms as the principal nucleophilic sites. The main positive values occur at C19 (+0.365), C3 (+0.358), and C13 (+0.344), with C19 representing the dominant electrophilic site.

3.3.2. Dual Reactivity Descriptors and Molecular Electrostatic Potential of Compound 2

Table 5 presents the local and dual reactivity descriptors calculated for the optimized structure of compound 2 using Natural Population Analysis (NPA) at the B3LYP/6-311G (d, p) level of theory. The corresponding profile of the dual descriptor Δf is shown in *Figure 5*, while *Figure 6* displays the molecular electrostatic potential (MEP) surface of the compound. In the MEP map, regions with predominantly nucleophilic character are shown in red, whereas regions with predominantly electrophilic character are shown in blue.

Table 5. *Local and dual reactivity descriptors of compound 2 calculated from NPA at the B3LYP/6-311G (d, p) level of theory.*

Atoms	Local descriptors						Dual descriptors		
	f+	f-	Atoms	f+	f-	Atoms	f+	f-	Atoms
C1	0,159	-0,149	0,076	-0,071	0,566	-0,528	0,308	0,147	1,094
C2	-0,136	0,161	-0,065	0,077	-0,484	0,570	-0,297	-0,142	-1,054
C3	0,192	-0,167	0,091	-0,080	0,680	-0,593	0,358	0,171	1,273
C4	-0,101	0,300	-0,048	0,143	-0,358	1,066	-0,401	-0,192	-1,424
C5	-0,109	0,014	-0,052	0,007	-0,388	0,049	-0,123	-0,059	-0,437
C6	-0,128	0,345	-0,061	0,165	-0,456	1,227	-0,474	-0,226	-1,682
O11	-0,325	0,427	-0,155	0,204	-1,154	1,515	-0,752	-0,359	-2,669
C13	0,107	-0,237	0,051	-0,113	0,381	-0,842	0,344	0,164	1,222
C14	-0,316	0,319	-0,151	0,152	-1,123	1,132	-0,635	-0,303	-2,255
N18	-0,306	0,453	-0,146	0,216	-1,087	1,607	-0,759	-0,362	-2,694
C19	0,166	-0,199	0,079	-0,095	0,589	-0,707	0,365	0,174	1,296
C20	-0,117	0,207	-0,056	0,099	-0,416	0,735	-0,324	-0,155	-1,150
C21	0,056	-0,019	0,027	-0,009	0,199	-0,067	0,075	0,036	0,267
C22	-0,069	0,057	-0,033	0,027	-0,246	0,203	-0,126	-0,060	-0,448
C24	-0,143	0,239	-0,068	0,114	-0,507	0,850	-0,382	-0,183	-1,357
O27	-0,320	0,392	-0,153	0,187	-1,138	1,390	-0,712	-0,340	-2,528
N28	-0,267	0,280	-0,127	0,134	-0,947	0,995	-0,547	-0,261	-1,942

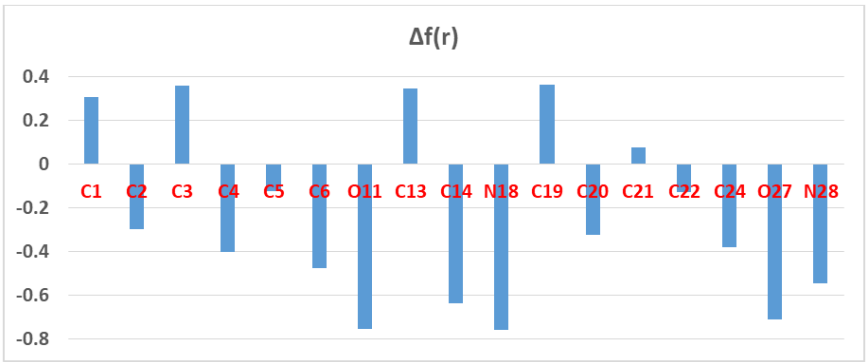

Figure 5. *Dual descriptor (Δf) profile of compound 2.*

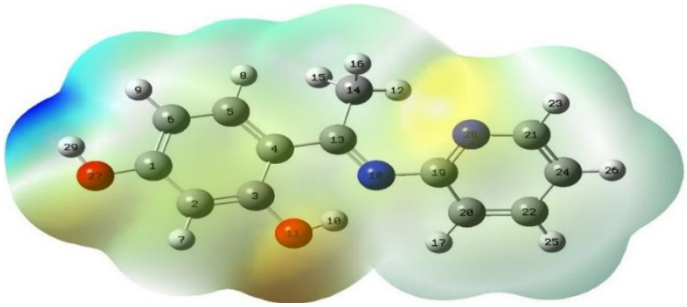

Figure 6. Molecular electrostatic potential surface of compound 2.

In compound 2, the N18 atom of the azomethine group exhibits the highest nucleophilic character, followed by the O11 and O27 oxygen atoms of the two hydroxyl groups on the phenyl ring. These two oxygen atoms, corresponding to the ortho- and para-hydroxyl substituents, respectively, constitute the other major nucleophilic sites. The presence of the second hydroxyl group, particularly O27, places the N28 atom of the pyridine ring in fourth position among the nucleophilic sites, with a noticeably lower nucleophilic character than the three main sites.

Among the electrophilic sites, the C19 carbon atom of the pyridine ring exhibits the strongest electrophilic character, followed by the C3 and C1 carbon atoms of the phenyl ring. These carbon atoms therefore represent the main sites likely to participate in interactions with nucleophilic species.

3.3.3. Dual Reactivity Descriptors and Molecular Electrostatic Potential of Compound 3

In compound 3, N18 remains the principal nucleophilic site, followed by O11 and the methoxy oxygen O27. The main electrophilic sites are C19, C3, and C13. Relative to compound 2, the methoxy substituent changes the local contribution of O27 without displacing the azomethine nitrogen from the first position.

Table 6. Local and dual reactivity descriptors of compound 3 calculated from NPA at the B3LYP/6-311G (d, p) level of theory.

Atoms	Local descriptors						Dual descriptors		
	f+	f-	Atoms	f+	f-	Atoms	f+	f-	Atoms
C1	0,159	-0,139	0,076	-0,066	0,557	-0,486	0,298	0,143	1,043
C2	-0,132	0,153	-0,063	0,073	-0,464	0,534	-0,285	-0,137	-0,997
C3	0,190	-0,173	0,091	-0,083	0,666	-0,604	0,363	0,174	1,270
C4	-0,102	0,304	-0,049	0,146	-0,355	1,064	-0,406	-0,194	-1,419
C5	-0,110	0,014	-0,053	0,007	-0,384	0,048	-0,123	-0,059	-0,432
C6	-0,133	0,350	-0,064	0,168	-0,465	1,224	-0,483	-0,231	-1,689
O11	-0,326	0,418	-0,156	0,200	-1,141	1,461	-0,743	-0,356	-2,602
C13	0,109	-0,239	0,052	-0,115	0,381	-0,837	0,348	0,167	1,218
C14	-0,316	0,319	-0,152	0,153	-1,107	1,116	-0,635	-0,304	-2,223
N18	-0,307	0,453	-0,147	0,217	-1,076	1,585	-0,760	-0,364	-2,660
C19	0,167	-0,202	0,080	-0,097	0,583	-0,706	0,368	0,177	1,289
C20	-0,118	0,204	-0,056	0,098	-0,412	0,713	-0,321	-0,154	-1,125
C21	0,056	-0,021	0,027	-0,010	0,195	-0,073	0,077	0,037	0,268
C22	-0,069	0,058	-0,033	0,028	-0,241	0,204	-0,127	-0,061	-0,445
C24	-0,143	0,235	-0,068	0,113	-0,499	0,824	-0,378	-0,181	-1,323
O27	-0,253	0,331	-0,121	0,159	-0,887	1,157	-0,584	-0,280	-2,044

Atoms	Local descriptors						Dual descriptors		
	f+	f-	Atoms	f+	f-	Atoms	f+	f-	Atoms
N28	-0,266	0,280	-0,128	0,134	-0,932	0,980	-0,546	-0,262	-1,912
C29	-0,103	0,090	-0,049	0,043	-0,359	0,316	-0,193	-0,092	-0,675

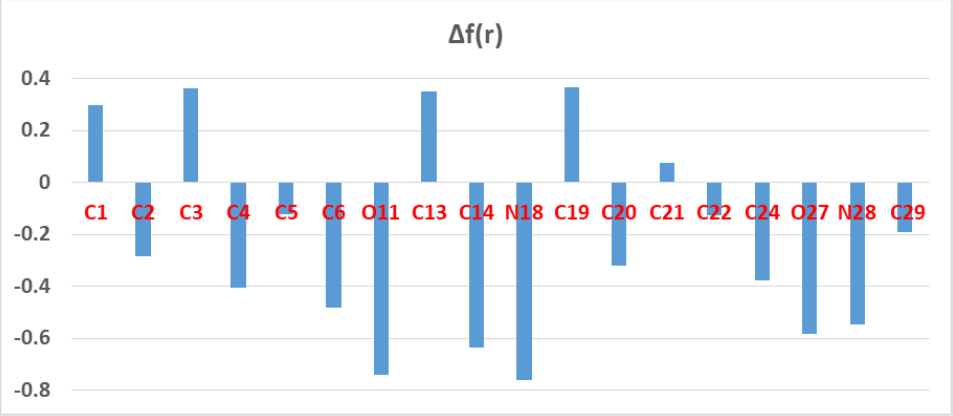

Figure 7. *Dual descriptor (Δf) profile of compound 3.*

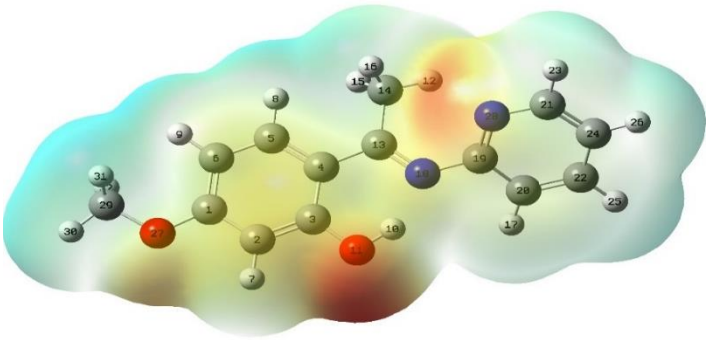

Figure 8. *Molecular electrostatic potential surface of compound 3.*

In compound 3, the N18 atom of the azomethine group exhibits the highest nucleophilic character, followed by the phenolic oxygen atom O11. The O27 atom, corresponding to the ether oxygen of the methoxy substituent (–OCH_3) at position 5 of the phenyl ring, ranks as the third most nucleophilic site. This methoxy group is para to the azomethine-derived substituent at position 2 of the phenyl ring. Compared with compound 2, the introduction of the methoxy substituent appears to modify the local nucleophilic character of O27.

The C19 carbon atom of the pyridine ring is identified as the most electrophilic site in compound 3, followed by the C3 carbon atom of the phenyl ring. The C13 carbon atom of the phenyl ring ranks third among the most electrophilic sites.

3.3.4. Dual Reactivity Descriptors and Molecular Electrostatic Potential of Compound 4

Compound 4 shows the clearest change in nucleophilic-site ranking: O11 is the most nucleophilic site, followed by N18, C30, and N28. C19 and C3 remain the principal electrophilic sites. The negative Δf value at C30 should be interpreted cautiously because it represents a saturated carbon atom rather than a conventional heteroatom-based nucleophilic centre.

Table 7. Local and dual reactivity descriptors of compound 4 calculated from NPA at the B3LYP/6-311G (d, p) level of theory.

Atoms	Local descriptors						Dual descriptors		
	f+	f-	Atoms	f+	f-	Atoms	f+	f-	Atoms
C1	-0,111	0,090	-0,054	0,044	-0,413	0,334	-0,201	-0,097	-0,747
C2	-0,109	0,186	-0,053	0,090	-0,407	0,690	-0,295	-0,143	-1,097
C3	0,181	-0,118	0,087	-0,057	0,671	-0,437	0,298	0,144	1,108
C4	-0,094	0,211	-0,046	0,102	-0,350	0,784	-0,305	-0,148	-1,134
C5	-0,114	0,038	-0,055	0,018	-0,422	0,141	-0,152	-0,073	-0,563
C6	-0,086	0,292	-0,042	0,141	-0,320	1,085	-0,378	-0,183	-1,404
O11	-0,326	0,477	-0,158	0,231	-1,213	1,773	-0,803	-0,389	-2,986
C13	0,115	-0,216	0,055	-0,105	0,426	-0,803	0,331	0,160	1,229
C14	-0,317	0,319	-0,154	0,155	-1,180	1,187	-0,637	-0,308	-2,367
N18	-0,304	0,403	-0,147	0,195	-1,131	1,498	-0,707	-0,343	-2,629
C19	0,171	-0,190	0,083	-0,092	0,635	-0,705	0,360	0,175	1,339
C20	-0,121	0,222	-0,059	0,108	-0,450	0,827	-0,343	-0,166	-1,276
C21	0,144	-0,095	0,070	-0,046	0,536	-0,354	0,240	0,116	0,890
C22	-0,066	0,049	-0,032	0,024	-0,245	0,184	-0,115	-0,056	-0,429
C24	-0,141	0,249	-0,068	0,121	-0,523	0,927	-0,390	-0,189	-1,450
N28	-0,278	0,274	-0,135	0,132	-1,033	1,017	-0,551	-0,267	-2,050
C30	-0,301	0,292	-0,146	0,141	-1,121	1,086	-0,594	-0,287	-2,206

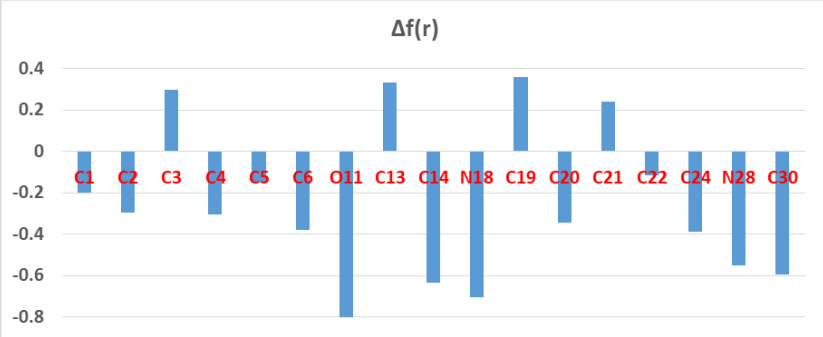

Figure 9. Dual descriptor (Δf) profile of compound 4.

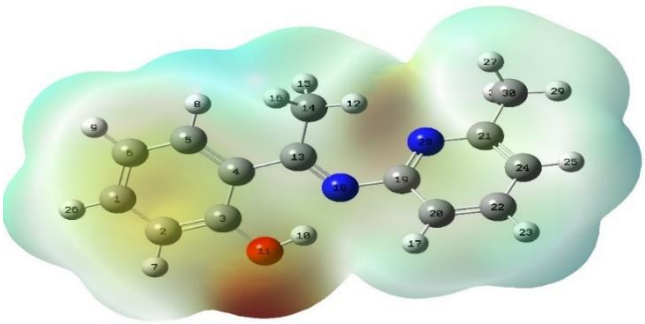

Figure 10. Molecular electrostatic potential surface of compound 4.

In the molecule (E)-2-(1-((6-methylpyridin-2-yl) imino)ethyl)phenol, the O11 oxygen atom of the phenyl group is identified as the most nucleophilic site, unlike the trend observed for the other compounds discussed above. The N18 atom of the azomethine group follows at a relatively large distance, indicating a markedly lower nucleophilic character. The C30 carbon atom of the methyl group attached to the pyridine ring ranks third, whereas the N28 atom of the pyridine ring occupies the fourth position among the nucleophilic sites.

Regarding electrophilicity, the C19 carbon atom of the pyridine ring remains the most electrophilic site in the molecule, followed by the C3 carbon atom of the phenyl ring. These results indicate that the introduction of the methyl substituent modifies the relative strength of the main nucleophilic sites while leaving the principal electrophilic center essentially unchanged.

3.3.5. Dual Reactivity Descriptors and Molecular Electrostatic Potential of Compound 5

In compound 5, N18 is the main nucleophilic site, followed by the oxygen centres O11 and O27. The main electrophilic sites remain C19, C3, and C13. Thus, the additional hydroxyl and methyl substituents mainly modify the relative magnitude of local reactivity while preserving the dominant electrophilic centre.

Table 8. *Local and dual reactivity descriptors of compound 5 calculated from NPA at the B3LYP/6-311G (d, p) level of theory.*

Atoms	Local descriptors						Dual descriptors		
	f+	f-	Atoms	f+	f-	Atoms	f+	f-	Atoms
C1	0,159	-0,149	0,076	-0,071	0,549	-0,516	0,308	0,147	1,064
C2	-0,136	0,161	-0,065	0,076	-0,471	0,555	-0,297	-0,141	-1,026
C3	0,191	-0,169	0,091	-0,081	0,661	-0,585	0,361	0,172	1,246
C4	-0,101	0,286	-0,048	0,136	-0,348	0,988	-0,387	-0,184	-1,336
C5	-0,110	0,019	-0,052	0,009	-0,379	0,066	-0,129	-0,061	-0,445
C6	-0,129	0,332	-0,061	0,158	-0,444	1,147	-0,461	-0,219	-1,591
O11	-0,325	0,421	-0,155	0,200	-1,123	1,454	-0,746	-0,355	-2,577
C13	0,107	-0,232	0,051	-0,110	0,370	-0,801	0,339	0,161	1,171
C14	-0,316	0,319	-0,150	0,152	-1,092	1,102	-0,635	-0,302	-2,194
N18	-0,305	0,444	-0,145	0,211	-1,055	1,535	-0,749	-0,357	-2,590
C19	0,170	-0,199	0,081	-0,095	0,588	-0,689	0,369	0,176	1,276
C20	-0,120	0,229	-0,057	0,109	-0,415	0,791	-0,349	-0,166	-1,206
C21	0,145	-0,100	0,069	-0,048	0,500	-0,345	0,245	0,116	0,845
C22	-0,068	0,047	-0,032	0,023	-0,234	0,164	-0,115	-0,055	-0,398
C24	-0,144	0,256	-0,068	0,122	-0,496	0,886	-0,400	-0,190	-1,382
O27	-0,321	0,388	-0,153	0,185	-1,108	1,342	-0,709	-0,338	-2,450
N28	-0,281	0,281	-0,134	0,134	-0,971	0,973	-0,562	-0,268	-1,943
C30	-0,301	0,292	-0,144	0,139	-1,042	1,009	-0,593	-0,283	-2,050

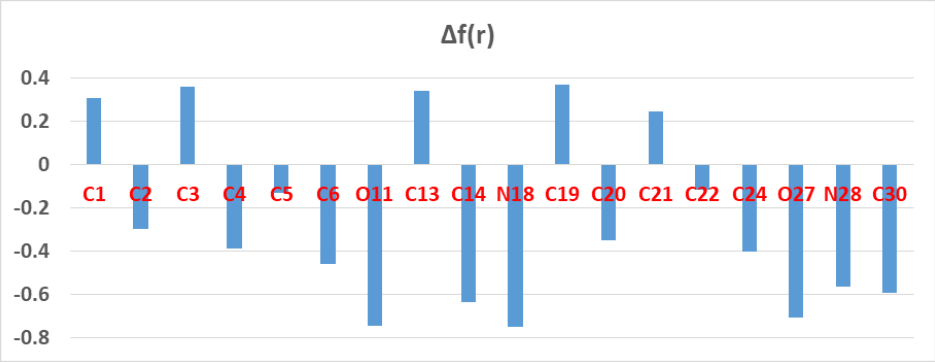

Figure 11. *Dual descriptor (Δf) profile of compound 5.*

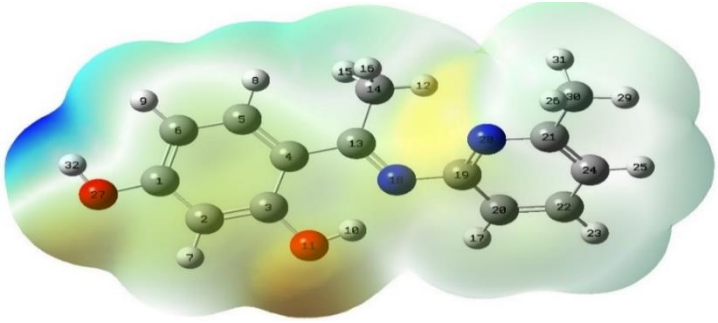

Figure 12. *Molecular electrostatic potential surface of compound 5.*

For compound 5, (E)-4-(1-((6-methylpyridin-2-yl)imino)ethyl)benzene-1,3-diol, the N18 atom of the azomethine group exhibits the highest nucleophilic character. It is followed, with relatively small differences, by the O11 and O27 oxygen atoms, as well as by the ortho- and para-related sites on the phenyl ring. Far below these main nucleophilic sites are the C30 carbon atom of the methyl group attached to the pyridine ring and the N28 nitrogen atom of the pyridine ring, which display comparatively weaker nucleophilic character.

With regard to electrophilicity, the C19 carbon atom of the pyridine ring is identified as the most electrophilic site in compound 5. It is followed by the C3 and C13 carbon atoms of the phenyl ring, which also show appreciable electrophilic character.

3.3.6. Dual Reactivity Descriptors and Molecular Electrostatic Potential of Compound 6

The local and dual reactivity descriptors of the optimised compound 6 were calculated from Natural Population Analysis (NPA) at the B3LYP/6-311G (d, p) level of theory. The results are summarised in Table 9. The profile of the dual descriptor, (Δf), is presented in Figure 13, while the molecular electrostatic potential surface of compound 6 is shown in Figure 14.

Table 9. *Local and dual reactivity descriptors of compound 6 calculated from NPA at the B3LYP/6-311G (d, p) level of theory.*

Atoms	Local descriptors						Dual descriptors		
	f+	f-	S+	S-	ω+	ω-	Δf(r)	ΔS(r)	ΔW(r)
C1	0.159	-0.140	0.076	-0.067	0.541	-0.476	0.298	0.143	1.018
C2	-0.133	0.153	-0.063	0.073	-0.452	0.522	-0.285	-0.137	-0.974
C3	0.190	-0.174	0.091	-0.083	0.649	-0.595	0.364	0.174	1.244
C4	-0.101	0.290	-0.048	0.139	-0.346	0.990	-0.391	-0.187	-1.336
C5	-0.110	0.019	-0.053	0.009	-0.376	0.064	-0.129	-0.062	-0.440

Atoms	Local descriptors						Dual descriptors		
	f+	f-	S+	S-	ω+	ω-	Δf(r)	ΔS(r)	ΔW(r)
C6	-0.133	0.337	-0.064	0.161	-0.455	1.150	-0.470	-0.225	-1.604
O11	-0.326	0.413	-0.156	0.197	-1.113	1.409	-0.739	-0.353	-2.522
C13	0.109	-0.234	0.052	-0.112	0.371	-0.799	0.343	0.164	1.170
C14	-0.316	0.319	-0.151	0.152	-1.079	1.088	-0.635	-0.304	-2.167
N18	-0.306	0.445	-0.147	0.213	-1.045	1.519	-0.751	-0.359	-2.564
C19	0.171	-0.202	0.082	-0.097	0.583	-0.689	0.373	0.178	1.273
C20	-0.121	0.225	-0.058	0.108	-0.412	0.768	-0.346	-0.165	-1.179
C21	0.144	-0.102	0.069	-0.049	0.493	-0.349	0.247	0.118	0.842
C22	-0.067	0.049	-0.032	0.023	-0.230	0.166	-0.116	-0.056	-0.396
C24	-0.144	0.252	-0.069	0.120	-0.490	0.859	-0.396	-0.189	-1.350
O27	-0.254	0.326	-0.121	0.156	-0.865	1.114	-0.580	-0.277	-1.979
N28	-0.281	0.282	-0.134	0.135	-0.958	0.963	-0.563	-0.269	-1.920
C29	-0.103	0.091	-0.049	0.043	-0.350	0.309	-0.193	-0.092	-0.659
C30	-0.301	0.292	-0.144	0.140	-1.028	0.997	-0.593	-0.284	-2.025

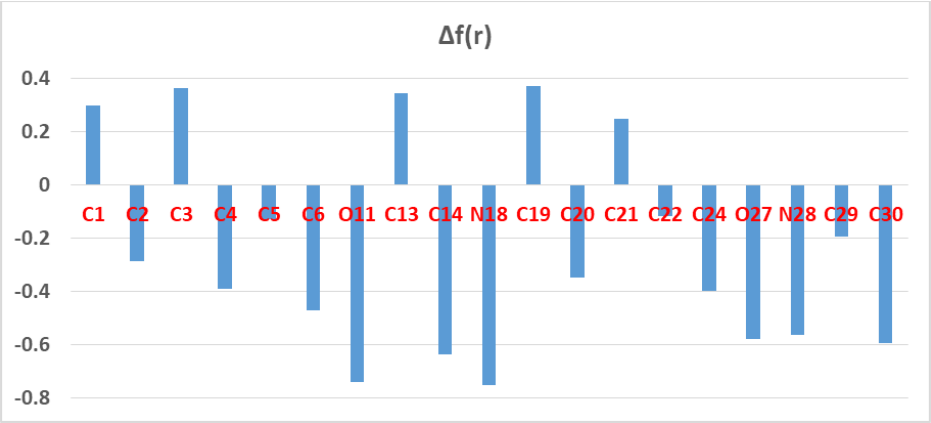

Figure 13. *Dual descriptor (Δf) profile of compound 6.*

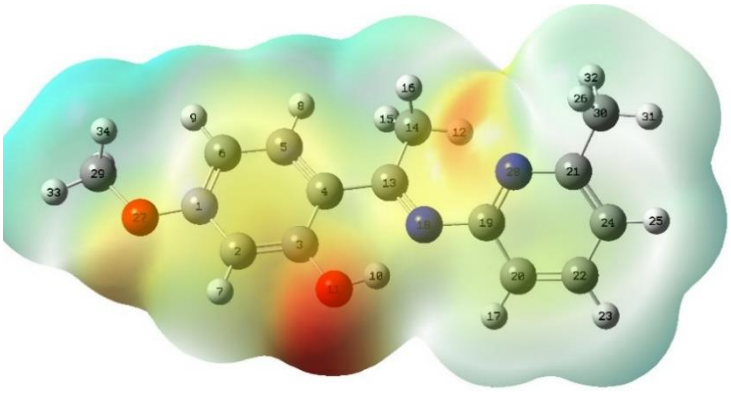

Figure 14. *Molecular electrostatic potential surface of compound 6.*

Compound 6 corresponds to (E)-5-methoxy-2-(1-((6-methylpyridin-2-yl)imino)ethyl)phenol. The data in Table 9 show that N18 (Δf = −0.751) and O11 (Δf = −0.739) remain the two main nucleophilic sites. O27 (−0.580) and N28 (−0.563) also show appreciable negative Δf values.

The C30 atom of the methyl substituent also gives a negative Δf value (−0.593). As discussed for compound 4, this value should be interpreted as a relative local nucleophilic character rather than as evidence of conventional nucleophilic reactivity of a saturated carbon atom.

This distinction is important because the negative Δf value at C30 reflects the calculated redistribution of electron density, whereas heteroatom sites such as N18, O11, O27, and N28 can be discussed more directly in terms of available lone-pair electron density.

The main electrophilic sites are C19, C3, and C13, with Δf values of +0.373, +0.364, and +0.343, respectively. C19 therefore remains the dominant electrophilic site, followed by C3 and C13.

The persistence of C19 as the principal electrophilic site is consistent with its electronic environment near the two nitrogen centres, N18 and N28, which contributes to local electron deficiency.

The positive Δf values at C3 and C13 indicate additional electron-deficient regions on the phenyl ring; their relative magnitudes can be influenced by the hydroxyl and methoxy substituents and by conjugation within the aromatic system.

3.4. Comparative Analysis of the Reactive Sites in Compounds 1–6

The six compounds share a common reactivity framework, but the substituents modify the relative magnitude and ranking of the local descriptors. Table 10 makes this pattern explicit and shows that the changes are more pronounced for nucleophilic sites than for electrophilic sites.

Compound 1 provides the reference pattern, with N18 > O11 > N28 on the nucleophilic side and C19 > C3 > C13 on the electrophilic side.

Adding a second hydroxyl group in compound 2 introduces O27 as an important nucleophilic site (N18 > O11 > O27 > N28), while C19 remains the main electrophilic site. The principal change is therefore the strengthening and multiplication of oxygen-based nucleophilic centres.

For compound 3, the methoxy oxygen O27 is also among the main nucleophilic sites (N18 > O11 > O27), but the electrophilic sequence remains C19 > C3 > C13. This indicates a local electronic effect without a change in the dominant electrophilic centre.

Compound 4 differs most clearly in nucleophilic ranking, with O11 > N18 > C30 > N28. Despite this change, C19 > C3 remains the principal electrophilic sequence. The C30 result should be regarded as a relative descriptor trend rather than conventional carbon-centred nucleophilicity.

Compounds 5 and 6 recover N18 as the leading nucleophilic site. In compound 5, the two hydroxyl-related oxygen centres are prominent, whereas compound 6 combines O11 and methoxy O27 as the main oxygen-based sites. Both retain C19 > C3 > C13 on the electrophilic side.

Two general trends therefore emerge. First, N18 and O11 form a persistent nucleophilic core, with O27 becoming important when an additional oxygen-containing substituent is present. Second, C19 is consistently the dominant electrophilic site across all six compounds, followed by selected phenyl-ring carbon atoms.

The substituents consequently act mainly by tuning the intensity and relative ranking of local reactivity. Hydroxyl substitution introduces a strongly electron-rich oxygen centre; methoxy substitution produces a related but distinct effect at O27; and methyl substitution perturbs the ranking of the existing heteroatom sites, most clearly in compound 4.

These local changes occur against a relatively stable global electronic background: the HOMO–LUMO gaps span only 4.112–4.201 eV, while hardness, softness, and electrophilicity also vary moderately. The combined analysis therefore indicates that substitution fine-tunes local electron-density distribution more than it changes the fundamental electronic framework.

The agreement among the frontier-orbital results, global descriptors, dual descriptors, NPA-derived populations, and MEP maps supports a coherent interpretation of the series: the ketimine framework largely preserves the identity of the principal reactive regions, whereas substituents modulate their relative strength.

The comparative ranking of the principal nucleophilic and electrophilic sites identified in compounds 1–6 is summarized in Table 10.

Table 10. *Comparative ranking of the main nucleophilic and electrophilic sites in compounds 1–6.*

Compound	Main nucleophilic sites	Main electrophilic sites	Main substituent effect
1	N18 > O11 > N28	C19 > C3 > C13	Reference structure
2	N18 > O11 > O27 > N28	C19 > C3 > C1	Additional –OH introduces a strong nucleophilic O site
3	N18 > O11 > O27	C19 > C3 > C13	–OCH_3 modifies the nucleophilicity of O27

Compound	Main nucleophilic sites	Main electrophilic sites	Main substituent effect
4	O11 > N18 > C30 > N28	C19 > C3	$–CH_3$ changes the relative ranking of nucleophilic sites
5	N18 > O11 > O27	C19 > C3 > C13	–OH + $–CH_3$ preserves the main reactive framework
6	N18 > O11 > O27	C19 > C3 > C13	$–OCH_3$ + $–CH_3$ mainly changes descriptor magnitudes

Table 10 shows that the principal reactive sites are largely conserved across compounds 1–6. C19 is the main electrophilic site in every compound, although C1 replaces C13 among the principal sites in compound 2 and the ranking of the nucleophilic sites changes more noticeably. N18 and O11 form the most persistent nucleophilic pair, while O27 becomes prominent when hydroxyl or methoxy substitution introduces an additional oxygen centre. Compound 4 is the main exception in ranking, with O11 preceding N18 and C30 appearing among the calculated negative-Δf sites. Overall, the substituents mainly modulate the magnitude and relative ranking of local reactivity rather than relocating the dominant electrophilic centre.

Overall, these findings are consistent with the trends reported in the literature, supporting the reliability of conceptual DFT as a useful framework for describing and interpreting molecular reactivity.

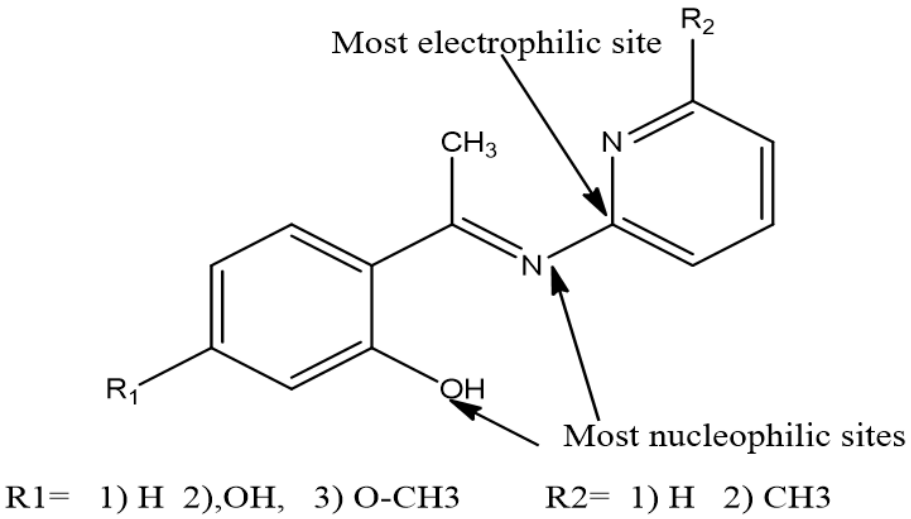

Figure 15. *Nucleophilic and electrophilic sites of the compounds.*

4. Conclusion

This study focused on the theoretical analysis of the electronic properties and reactivity of six Schiff base compounds using quantum chemical methods. The results show that all six molecules exhibit relatively large HOMO–LUMO energy gaps, indicating appreciable electronic stability. The analysis of the global reactivity descriptors also revealed moderate differences in ionisation potential, chemical hardness, softness, and electrophilicity, highlighting the modulation of electronic reactivity according to molecular structure.

The analysis of the Fukui functions and the dual descriptor made it possible to identify the main sites likely to participate in chemical interactions. Nitrogen and oxygen atoms were primarily associated with regions exhibiting nucleophilic character, whereas certain carbon atoms constituted the preferred sites for electrophilic interactions. Molecular electrostatic potential maps generally confirmed the distribution of electron-rich and electron-deficient regions.

Overall, the results indicate that the structural substitutions investigated modify the intensity of the electronic properties without causing major changes in the principal reactive sites. The originality of this work therefore lies in relating the global electronic properties to the local reactivity of this series of compounds, providing useful theoretical insights to guide further experimental investigations and potential applications. Further studies, particularly those involving TD-DFT calculations, investigations of interactions with biological targets, and experimental validation, could provide deeper insight into these findings.

Abbreviations

HOMO	Highest Occupied Molecular Orbital
LUMO	Lowest Unoccupied Molecular Orbital
DFT	Density Functional Theory
TD-DFT	Time-Dependent Density Functional Theory
MEP	Molecular Electrostatic Potential
NPA	Natural Population Analysis
CDFT	Conceptual Density Functional Theory
ICT	Intramolecular Charge Transfer

Author Contributions

Niamké Jean Baptiste Kangah: Conceptualization, Resources

Siriki Doumbia: Conceptualization, Resources

Clémence Ingrid Bléhoué: Conceptualization, Resources

Georges Stephane Dembélé: Conceptualization, Resources

Wawohinlin Patrice Ouattara: Data curation, Methodology

Bibata Konaté: Data curation, Methodology

Nanou Tieba Tuo: Data curation, Methodology

Mamadou Guy Richard Koné: Conceptualization, Resources

Charles Guillaume Kodjo: Data curation, Methodology

Conflicts of Interest

The authors declare no conflicts of interest.

References

[1] Layer RW. The chemistry of imines. Chem Rev. 1963; 63: 489-510. https://doi.org/10.1021/cr60225a003

[2] Mushtaq I, Ahmad M, Saleem M, et al. Pharmaceutical significance of Schiff bases: an overview. Future J Pharm Sci. 2024; 10: 16. https://doi.org/10.1186/s43094-024-00594-5

[3] Nidhi, Siddharam S, Rao DP, Gautam AK, Verma A, Azad CS. Schiff bases and their possible therapeutic applications: a review. Results Chem. 2025; 13: 101941. https://doi.org/10.1016/j.rechem.2024.101941

[4] Ceylan Ü, Çapan A, Yalçın ŞP, Sönmez M, Aygün M. Vibrational spectroscopic and thermodynamical property studies, Fukui functions, HOMO-LUMO, NLO, NBO and crystal structure analysis of a new Schiff base bearing phenoxy-imine group. J Mol Struct. 2017; 1136: 222-230. https://doi.org/10.1016/j.molstruc.2017.02.014

[5] Ejiah FN, Rofiu MO, Oloba-Whenu OA, Fasina TM. Schiff bases as analytical tools: synthesis, chemo-sensor, and computational studies of 2-aminophenol Schiff bases. Mater Adv. 2023; 4: 2308-2321. https://doi.org/10.1039/D3MA00097D

[6] Parr RG, Yang W. Density-functional approach to the frontier-electron theory of chemical reactivity. J Am Chem Soc. 1984; 106: 4049-4050. https://doi.org/10.1021/ja00326a036

[7] Chakraborty D, Chattaraj PK. Conceptual density functional theory based electronic structure principles. Chem Sci. 2021; 12: 6264-6279. https://doi.org/10.1039/D0SC07017C

[8] Pucci R, Angilella GGN. Density functional theory, chemical reactivity, and the Fukui functions. Found Chem. 2022; 24: 59-71. https://doi.org/10.1007/s10698-022-09416-z

[9] Parr RG, Szentpály LV, Liu S. Electrophilicity index. J Am Chem Soc. 1999; 121: 1922-1924. https://doi.org/10.1021/ja983494x

[10] Yang W, Parr RG, Pucci R. Electron density, Kohn-Sham frontier orbitals, and Fukui functions. J Chem Phys. 1984; 81: 2862-2863. https://doi.org/10.1063/1.447964

[11] Morell C, Grand A, Toro-Labbé A. New dual descriptor for chemical reactivity. J Phys Chem A. 2005; 109: 205-212. https://doi.org/10.1021/jp046577a

[12] Kosar B, Albayrak C. Spectroscopic investigations and quantum chemical computational study of (E)-4-methoxy-2-[(p-tolylimino) methyl] phenol. Spectrochim Acta A Mol Biomol Spectrosc. 2011; 78: 160-167. https://doi.org/10.1016/j.saa.2010.09.016

[13] Reed AE, Weinstock RB, Weinhold F. Natural population analysis. J Chem Phys. 1985; 83: 735-746. https://doi.org/10.1063/1.449486

[14] Akbari Z, Stagno C, Iraci N, Efferth T, Omer EA, Piperno A, et al. Biological evaluation, DFT, MEP, HOMO-LUMO analysis and ensemble docking studies of Zn (II) complexes of bidentate and tetradentate Schiff base ligands as antileukemia agents. J Mol Struct. 2024; 1301: 137400. https://doi.org/10.1016/j.molstruc.2023.137400

[15] M. J. Frisch, G. W. Trucks, H. B. Schlegel, G. E. Scuseria, M. A. Robb, J. R. Cheeseman, G. Scalmani, V. Barone, B. Mennuci, G. A. Petersson, H. Nakatsuji, M. Caricato, X. Li, H. P. Hratchian, A. F. Izmaylov, J. Bloino, G. Zheng, J. L. Sonnerberg, M. Hada, Ehara, K. Toyota, R. Fukuda, J. Hasegawa, M. Ishida, T. Nakajima, Y. Honda, O. Kitao, H. Nakai, T. Vreven, A. Montgomery, J. E. Peralta, F. Ogliaro, M. Bearpark, J. J. Heyd, E. Brothers, K. N. Kudin, V. N. Staroverov, R. Kobayashi, J. Normand, K. Raghavachari, A. Rendell, J. C. Burant, S. S. Iyengar, J. Tomasi, M. Cossi, N. Rega, J. M. Milliam, M. Klene, J. E. Knox, J. B. Cross, V. Bakken, C. Adamo, J. Jaramillo, R. Gomperts, R. E. stratmann, O. Yazyev, A. J. Austin, R. Cammi, C. Pomeli, J. W. Ochterski, R. L. Martin, K. Morokuma, V. G. Zakrzewski, G. A. Voth, P. Salvador, J. J. Dannenberg, S. Dapprich, S. Daniels, O. Farkas, J. B. Foresman, J. V. Ortiz, J. Cioslowski et D. J. Fox, Gaussian 09, Revison A. 02, WAllingford C T: inc, 2009.

[16] Pearson RG. Hard and soft acids and bases. J Am Chem Soc. 1963; 85: 3533-3539. https://doi.org/10.1021/ja00905a001

[17] Sinha L, Prasad O, Narayan V, Shukla SR. Raman, FT-IR spectroscopic analysis and first-order hyperpolarisability of 3-benzoyl-5-chlorouracil by first principles. Mol Simul. 2011; 37: 153-163. https://doi.org/10.1080/08927022.2010.533273

[18] Sustmann R. Orbital energy control of cycloaddition reactivity. Tetrahedron Lett. 1971; 12: 2717-2721. https://doi.org/10.1016/S0040-4039(01)96961-8

[19] Midoune A, Messaoud A. Étude computationnelle DFT/TD-DFT de la molécule tétrathiafulvalène-1, 3-benzothiazole pour mettre en évidence ses propriétés structurelles, électroniques, vibrationnelles et optiques non linéaires. C R Chim. 2020; 23: 143-158. https://doi.org/10.5802/crchim.12